JACS
JOURNAL OF THE AMERICAN CHEMICAL SOCIETY
Article
pubs.acs.org/JACS

Microhydration Effects on the Encapsulation of Potassium Ion by Dibenzo-18-Crown-6

Yoshiya Inokuchi,*[,†] Takayuki Ebata,[†] Thomas R. Rizzo,[‡] and Oleg V. Boyarkin[‡]

[†]Department of Chemistry, Graduate School of Science, Hiroshima University, Higashi-Hiroshima, Hiroshima 739-8526, Japan
[‡]Laboratoire de Chimie Physique Moléculaire, École Polytechnique Fédérale de Lausanne, Lausanne CH-1015, Switzerland

Supporting Information

ABSTRACT: We have measured electronic and conformer-specific vibrational spectra of hydrated dibenzo-18-crown-6 (DB18C6) complexes with potassium ion, K^+•DB18C6•$(H_2O)_n$ (n = 1−5), in a cold, 22-pole ion trap. We also present for comparison spectra of Rb^+•DB18C6•$(H_2O)_3$ and Cs^+•DB18C6•$(H_2O)_3$ complexes. We determine the number and the structure of conformers by analyzing the spectra with the aid of quantum chemical calculations. The K^+•DB18C6•$(H_2O)_1$ complex has only one conformer under the conditions of our experiment. For K^+•DB18C6•$(H_2O)_n$ with n = 2 and 3, there are at least two conformers even under the cold conditions, whereas Rb^+•DB18C6•$(H_2O)_3$ and Cs^+•DB18C6•$(H_2O)_3$ each exhibit only one isomer. The difference can be explained by the optimum matching in size between the K^+ ion and the crown cavity; because the K^+ ion can be deeply encapsulated by DB18C6 and the interaction between the K^+ ion and the H_2O molecules becomes weak, different kinds of hydration geometries can occur for the K^+•DB18C6 complex, giving multiple conformations in the experiment. For K^+•DB18C6•$(H_2O)_n$ (n = 4 and 5) complexes, only a single isomer is found. This is attributed to a cooperative effect of the H_2O molecules on the hydration of K^+•DB18C6; the H_2O molecules form a ring, which is bound on top of the K^+•DB18C6 complex. According to the stable structure determined in this study, the K^+ ion in the K^+•DB18C6•$(H_2O)_n$ complexes tends to be pulled largely out from the crown cavity by the H_2O molecules with increasing n. Multiple conformations observed for the K^+ complexes will have an advantage for the effective capture of the K^+ ion over the other alkali metal ions by DB18C6 because of entropic effects on the formation of hydrated complexes.

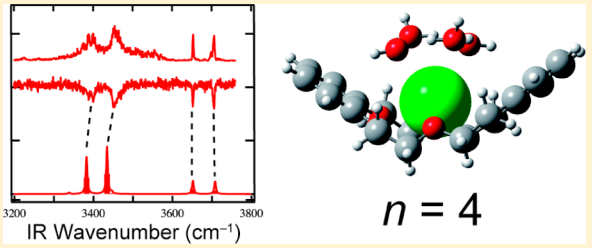

1. INTRODUCTION

Crown ethers are among the most common host molecules in supramolecular chemistry and are extensively used as phase transfer catalysts in organic synthesis. Despite their wide use, the origin of their functionality has not been fully understood at the molecular level. For example, 18-crown-6 (18C6) selectively captures K^+ in a water solution of different alkali metal ions.[1,2] This ability of selective encapsulation has been explained mainly in terms of optimal size matching between the cavity of crown ethers and guest species, based on X-ray analysis.[1,3] Focusing on the alkali metal ion−18C6 complexes, the ion selectivity can be expressed by the following metal exchange reaction:[4,5]

$$K^+ \bullet 18C6 + M^+ \rightleftharpoons M^+ \bullet 18C6 + K^+ \quad (1)$$

where M = Li, Na, K, Rb, and Cs. To evaluate the relative stability between the left- and right-hand sides of reaction 1, the stabilization energy of the M^+•18C6 complexes should be obtained. Experimentally, mass spectrometric, collision-induced dissociation, and ion mobility studies have been applied to alkali metal ion−crown ether complexes by Armentrout, Dearden, Brodbelt, Bowers, and their co-workers.[6−29] These gas-phase studies for the nonsolvated M^+•18C6 complexes demonstrate that the intrinsic affinity of 18C6 is controlled primarily by the ion charge density. The binding energy of the M^+•18C6 complexes thus ranges according to the ion size as $Li^+ > Na^+ > K^+ > Rb^+ > Cs^+$. This conclusion indicates that solvent plays a crucial role in the selectivity of K^+ ion in solution.[10−12,21] Armentrout and co-workers considered the possibility of multiple conformers to explain the discrepancy in binding energy for metal ion complexes with ether molecules between those observed and those calculated in the gas phase.[9,10] Kollman and co-workers suggested from their molecular mechanics (MM) calculations that the selectivity of K^+ over Na^+ by 18C6 in aqueous solution is due to the fact that the difference in hydration energies of Na^+ and K^+ is larger than the difference in stabilization energies of Na^+•18C6 and K^+•18C6.[30] Later, van Eerden et al.[31] and Dang[32] drew similar conclusions from their molecular dynamics (MD) studies. Accounting for microhydration of M^+ and M^+•18C6, reaction 1 can be written[4,5]

$$K^+ \bullet 18C6 + M^+ \bullet (H_2O)_m \rightleftharpoons M^+ \bullet 18C6 + K^+ \bullet (H_2O)_m \quad (2)$$

Received: August 19, 2013
Published: January 14, 2014

   dx.doi.org/10.1021/ja4086066 | J. Am. Chem. Soc. 2014, 136, 1815−1824

$$K^+ \bullet 18C6 \bullet (H_2O)_n + M^+ \bullet (H_2O)_m \rightleftharpoons M^+ \bullet 18C6 \bullet (H_2O)_n + K^+ \bullet (H_2O)_m \quad (3)$$

Armentrout and co-workers evaluated the enthalpy change of reaction 2 by using experimentally determined enthalpies of $M^+\bullet$18C6 and $M^+\bullet(H_2O)_m$, demonstrating that five and six H_2O molecules (m = 5 and 6) make the left-hand side of reaction 2 more stable for all the alkali metal ions.[10,11] Glendening, Feller, and Thompson reported ab initio studies of the complexes in reactions 2 and 3.[4,5] They extended their calculations to $M^+\bullet18C6\bullet(H_2O)_n$ with n = 1−6 and obtained the enthalpy change of reactions 2 and 3 based on the calculated enthalpies. For reaction 2, only four H_2O molecules (m = 4) change the ion selectivity to $K^+ > Rb^+ \approx Na^+ > Cs^+ > Li^+$, the same as that measured in water. For reaction 3, the addition of up to six water molecules to the $M^+\bullet$18C6 complexes drastically reduces the discrepancy between the measured and calculated enthalpy change for aqueous solutions. These experimental and theoretical studies both suggest that the net effects due to hydration of not only the M^+ ions but also the $M^+\bullet$18C6 complexes are of great importance for determining the ion binding selectivity in solution. It was also pointed out that entropic effects, which were missing in the above studies, should be included to fully understand the ion selectivity, because the encapsulation process remains endothermic simply by considering only the enthalpy contribution.[5,10,11] To examine the entropic contribution, one has to determine the structure of the complexes related to eqs 1−3, which would allow a precise evaluation of vibrational frequencies; Glendening et al. mentioned that low-frequency vibrations must be obtained to better than 10 cm^{-1} to obtain kcal/mol accuracy for the entropy.[4] In addition, the number of conformers will also affect the ion selectivity; the larger the number of conformations a specific complex adopts, the more favorable is its formation. Apart from X-ray diffraction analysis in crystals, there are only a few reports that determine structures of the alkali metal ion−18C6 complexes and their hydrated species at the atomic level with conformational resolution. Average conformations of the $M^+\bullet$18C6 complexes in the gas phase and in water have been determined from MM and MD studies.[30−38] The MD simulations in aqueous solution demonstrated that the Na^+ and K^+ ions are located at the center of mass of 18C6 in water, whereas the Rb^+ and Cs^+ ions are displaced from the center because of their larger size.[32−36] The $K^+\bullet$18C6 simulation in water showed that on average two H_2O molecules are coordinated to K^+, one each from above and below the crown center.[35,36] Ab initio studies of the hydrated $M^+\bullet$18C6 complexes also determined their stable conformations;[4,5] however, because the main purpose of these ab initio studies was to obtain thermochemical values related to ion selectivity, the conformational search of the $M^+\bullet18C6\bullet(H_2O)_n$ complexes was not sufficiently extensive. Experimentally, Poonia determined the position of a H_2O molecule in the crystal of alkali metal halide−crown ether complexes using X-ray analysis and IR spectroscopy; an H_2O molecule was considered to be metal-coordinated on top of the $K^+\bullet$18C6 complex.[39] Metal ion−crown ether complexes were also examined in water solutions by NMR, IR spectroscopy, and some other techniques, but the hydration structure of the complexes remained unclear.[40,41] More recently, the structure of alkali metal ion−crown ether complexes has been investigated in the gas phase by both IR[42−45] and UV spectroscopy.[46−51] However, only Rodriguez, Vaden, and Lisy have reported IR spectroscopy of *hydrated* $M^+\bullet$18C6 complexes in the gas phase.[52−54] These studies attribute the observed IR spectra to multiple isomers, but the number of conformations and their relative contributions to the spectra are not clear because of broad and congested spectral features.[52−54] We have recently reported highly resolved UV and IR spectra of alkali metal complexes with dibenzo-18-crown-6 (DB18C6), benzo-18-crown-6 (B18C6), and benzo-15-crown-5 (B15C5) in a cooled, 22-pole ion trap.[49−51] These benzo-crown ethers have not been studied as extensively as 18C6, but one advantage of using them is that they have very sharp vibronic bands in UV absorption under cold conditions.[49−51] Resolved vibronic bands enable us to distinguish different conformers and measure conformer-specific IR spectra. We found that the alkali metal ion complexes of DB18C6 and B18C6 have structures similar to the corresponding 18C6 complexes, despite the structural constraints due to the benzene rings.[49−51]

In the present work, we investigate the conformations of cold complexes of DB18C6 with the potassium ion and water, $K^+\bullet DB18C6\bullet(H_2O)_n$ (n = 1−5). We employ IR−UV double-resonance spectroscopy to measure conformer-selective infrared spectra of the cold species in the OH stretching (3200−3800 cm^{-1}) region. We determine the number and the structure of the conformers by comparing the observed IR spectra and those calculated by quantum chemical methods. Finally, we present the experimental and computational results for $Rb^+\bullet DB18C6\bullet(H_2O)_3$ and $Cs^+\bullet DB18C6\bullet(H_2O)_3$ complexes, demonstrating the uniqueness of the $K^+\bullet$DB18C6 complex.

2. EXPERIMENTAL AND COMPUTATIONAL METHODS

The details of our experimental approach have been given elsewhere.[49,55] Briefly, the $K^+\bullet DB18C6\bullet(H_2O)_n$ complexes are produced continuously at atmospheric pressure via nanoelectrospray of a solution containing potassium chloride and DB18C6 (~10 μM each) dissolved in methanol/water (~9:1 volume ratio). The parent ions of interest are mass-selected in a quadrupole mass filter and injected into a 22-pole radio frequency (RF) ion trap, which is cooled by a closed-cycle He refrigerator to 6 K. The trapped ions are cooled internally and translationally to ~10 K through collisions with cold He buffer gas,[49,55−57] which is pulsed into the trap. The trapped ions are then irradiated with a UV laser pulse, which causes some fraction of them to dissociate. The resulting charged photofragments, as well as the remaining parent ions, are released from the trap, mass-analyzed by a second quadrupole mass filter, and detected with a channeltron electron multiplier. Ultraviolet photodissociation (UVPD) spectra of parent ions are obtained by plotting the yield of a particular photofragment ion as a function of the wavenumber of the UV laser. For IR−UV double-resonance spectroscopy, the output pulse of an IR optical parametric oscillator (OPO) precedes the UV pulse by ~100 ns and counterpropagates collinearly with it through the 22-pole. Absorption of the IR light by the ions in a specific conformational state warms them up, reducing the net UV absorption by the ions in this conformer.[58] The wavenumber of the UV laser is fixed to a vibronic transition of this conformer for monitoring the conformer-selective IR-induced depletion of the UVPD yield, and the wavenumber of the OPO is scanned in the OH stretching region (3200−3800 cm^{-1}) while monitoring the number of fragment ions. IR−UV depletion spectra are obtained by plotting the yield of a particular photofragment as a function of the OPO wavenumber.

For geometry optimization of the $K^+\bullet DB18C6\bullet(H_2O)_n$ complexes, we first use a classical force field to find conformational minima. The initial conformational search is performed by using the mixed torsional search with low-mode sampling and the AMBER* force field as implemented in MacroModel v. 9.1.[59] Minimum-energy conformers

dx.doi.org/10.1021/ja4086066 | J. Am. Chem. Soc. 2014, 136, 1815−1824

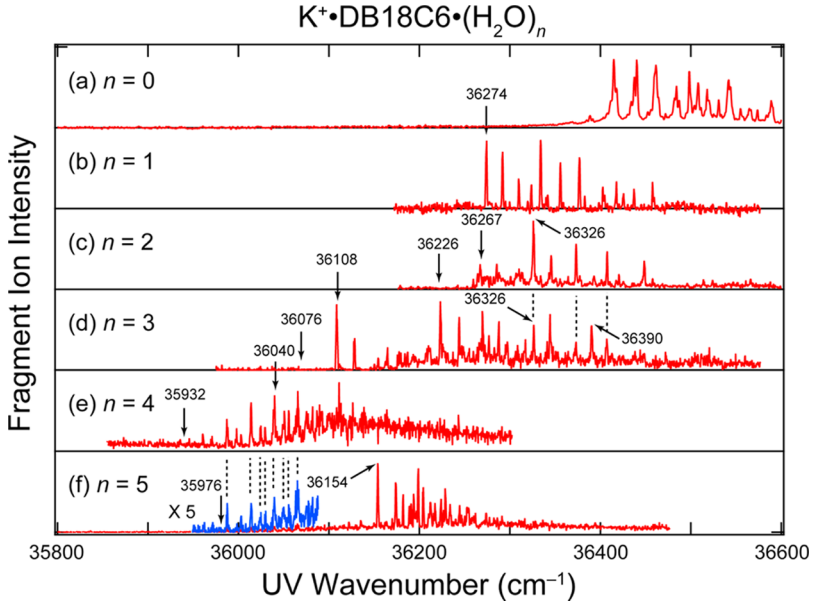

Figure 1. UVPD spectra of the K^+•DB18C6•$(H_2O)_n$ (n = 1−5) complexes with that of bare K^+•DB18C6 complex (ref 49). The arrows show the UV positions at which the IR−UV spectra are measured. The intensity of each spectrum is normalized as having the same maximum intensity for all the spectra.

found with the force field calculations are then optimized at the M05-2X/6-31+G(d) level with *loose* optimization criteria using the GAUSSIAN09 program package.[60] The unique minima obtained by comparison of relative energies and rotational constants are further optimized using combinations of the M05-2X or ωB97XD functional and 6-31+G(d) or 6-311++G(d,p) basis set. Vibrational analysis is carried out for the optimized structures at the same computational levels. Calculated frequencies at the M05-2X/6-31+G(d) level are scaled with a factor of 0.9525 for comparison with the IR−UV spectra. The IR spectra of a specific conformer calculated at different levels are similar to each other (see Figure 2S in the Supporting Information), whereas the relative stability of stable conformers depends on the employed level, especially for the n = 2 and 3 complexes. We therefore validate structures of the K^+•DB18C6•$(H_2O)_n$ complexes based on similarity of their observed and calculated IR spectra. All stable conformers are named systematically using "K1a" notation, where the first capital letter indicates the metal ion of a complex, the subsequent number represents the number of attached H_2O molecules, and the final lowercase letter stands for the stability order of conformers determined at the M05-2X/6-31+G(d) level with (nonscaled) zero-point energy correction. In the following figures, we also use nomenclature such as "K1a_1−0", which gives supplemental information on the hydration structure of the isomers; the first and second numbers indicate the number of water molecules on the top and bottom sides of the M^+•DB18C6 complexes, respectively. All the conformers with a total energy less than 5 kJ/mol relative to that of the most stable structure are shown in Figures 3S−7S of the Supporting Information.

3. RESULTS

Figure 1 shows the UVPD spectra of the cooled K^+•DB18C6•$(H_2O)_n$ (n = 0−5) complexes. The spectra for n > 0 are measured by monitoring the yield of the bare K^+•DB18C6 photofragment ion because it is a dominant photodissociation product and is hardly affected by the dissociation due to the metastable decay of the parent ions between the first quadrupole and the 22-pole ion trap. All the UVPD spectra in Figure 1 show a number of vibronically resolved bands. The origin band of bare K^+•DB18C6 is observed at 36 415 cm^{-1}.[49] All the K^+•DB18C6•$(H_2O)_n$ complexes show a red shift of the absorption relative to nonhydrated K^+•DB18C6. For the n = 1 complex, the origin band is found at 36 274 cm^{-1}. The n = 2 complex has a strong UV band at 36 326 cm^{-1}, and weak vibronic bands appear from 36 267 cm^{-1}. In the UVPD spectra of n = 3 and 5, the origin band clearly appears at 36 108 and 36 154 cm^{-1}, respectively. For the n = 4 ion, the UVPD spectrum is more congested than those of other complexes. As shown by dotted lines in parts d and f of Figure 1, the UVPD spectra of the n = 3 and 5 complexes contain weak features that seem to correspond to the vibronic bands of the n = 2 and 4 complexes, respectively. These bands could appear in the UV spectra via the evaporation of one H_2O molecule from the mass-selected n = 3 or 5 complex due to metastable decay of hot complexes after the first quadrupole or induced by collisions with He buffer gas in the 22-pole, followed by cooling and UV excitation. In the n = 4 spectrum, however, we cannot find any band due to the fragment n = 3 complex. These results imply that the n = 4 complex would have one substantially stable structure, which hardly dissociates by the metastable decay or by the collision with He, different from the case of the n = 3 and 5 ions.

We measure the IR−UV spectra of the K^+•DB18C6•$(H_2O)_n$ complexes by fixing the UV wavenumber at the positions pointed by the arrows in Figure 1 and scanning the wavenumber of the IR OPO. The IR−UV spectra recorded by fixing the UV frequency where there is no vibronic band provide IR gain spectra that are a sum of different conformers, if they exist.[50] We first measure IR gain spectra at nonresonant UV frequencies to see the IR absorption of all the conformers and then measure IR dip spectra with the UV fixed on specific vibronic bands to attribute IR bands to each conformer. Figure 2a displays the IR−UV spectrum of the n = 1 complex in the OH stretching region measured by monitoring the intensity of the origin band at 36 274 cm^{-1} in Figure 1b as the IR laser wavenumber is scanned. Vibrational bands are observed at 3715 and 3615 cm^{-1}. Parts b and c of Figure 2 show the calculated IR spectra of stable conformers (K1a and K1b) of the n = 1 complex; the structure of these conformers is illustrated in Figure 3a and Figure 3S in the Supporting Information. Since

dx.doi.org/10.1021/ja4086066 | J. Am. Chem. Soc. 2014, 136, 1815−1824

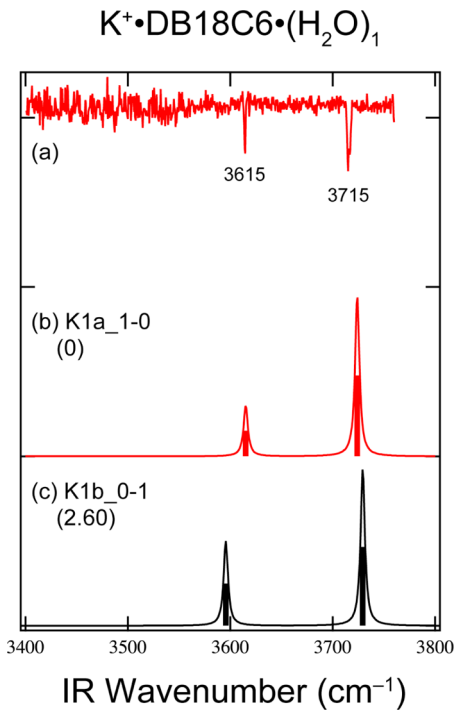

Figure 2. (a) IR–UV spectrum of the K^+•DB18C6•$(H_2O)_1$ complex measured at the UV wavenumber of 36 274 cm^{-1} (as shown with an arrow in Figure 1b). (b, c) IR spectra calculated for stable conformers (K1a and K1b). A scaling factor of 0.9525 is employed for the calculated vibrational frequencies. The numbers in parentheses show total energies (kJ/mol) relative to that of the most stable isomer (K1a).

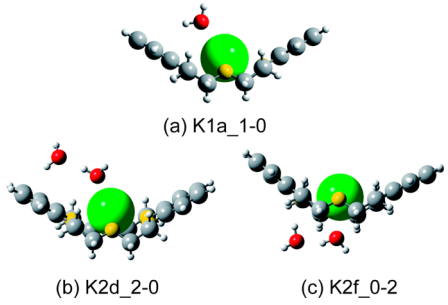

Figure 3. Structure of the n = 1 and 2 complexes determined by the comparison of the observed and calculated IR spectra. The crown oxygen atoms are shown in yellow to distinguish them from the water ones (red).

the calculated IR spectra of both K1a and K1b reproduce the observed IR bands well, one cannot determine the structure from the spectral comparison only. However, because K1a is more stable than K1b at all the calculation levels performed in this study by >2 kJ/mol, we attribute the structure of the n = 1 complex to K1a. The H_2O molecule in this structure is directly bound to the K^+ ion on top of K^+•DB18C6, and one OH group is H-bonded to one of the benzene rings. The vibrational analysis of K1a assigns the IR bands at 3715 and 3615 cm^{-1} to the antisymmetric and symmetric OH stretching vibrations of H_2O, respectively. The positions of the vibronic bands at which the IR spectra are observed, the IR band positions, and the conformer assignment are collected in Table 1.

Figure 4a–c displays the IR–UV spectra of the n = 2 ion measured with the UV laser fixed at 36 226, 36 326, and 36 267

Table 1. Positions of the UV Bands (cm^{-1}) at Which the IR–UV Spectra Have Been Measured, Positions of the IR–UV Bands (cm^{-1}), and Conformation Assignment of the K^+•DB18C6•$(H_2O)_n$ Complexes

n	UV band positions	IR band positions	conformer
1	36 274	3615, 3715	K1a
2	36 326	3452, 3601, ~3710, 3721	K2d
	36 267	3454, 3601, ~3720	K2f
3	36 108	3529, 3534, 3565, 3698, 3714	K3a
	(36 326)[a]	(3452)	(K2d)
	36 390	3463, 3602, 3711, 3720	K3g
4	36 040	~3400, ~3452, 3653, 3707	K4a
5	36 154	~3301, ~3364, ~3412, ~3438, ~3460, 3576, 3652, 3662, 3708, 3721	K5a

[a]This band originates from the n = 2 complex produced via evaporation of one H_2O molecule from the mass-selected n = 3 ion between the first quadrupole and the 22-pole.

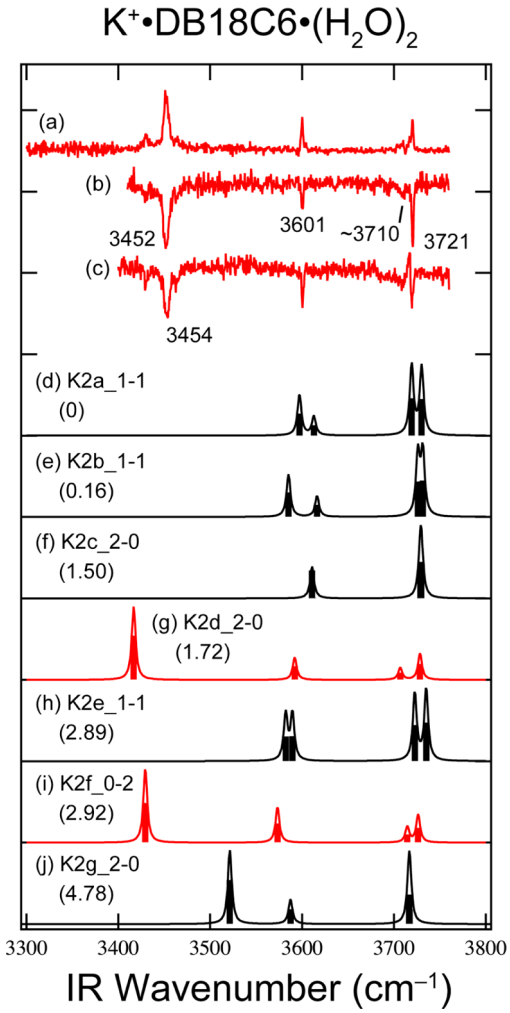

Figure 4. (a–c) IR–UV spectra of the K^+•DB18C6•$(H_2O)_2$ complex measured at the UV wavenumbers of 36 226, 36 326, and 36 267 cm^{-1}. The UV positions are shown with arrows in Figure 1c. (d–j) IR spectra calculated for stable conformers (K2a–K2g). A scaling factor of 0.9525 is employed for the vibrational frequencies calculated. The numbers in parentheses show total energies (kJ/mol) relative to that of the most stable isomer (K2a).

dx.doi.org/10.1021/ja4086066 | J. Am. Chem. Soc. 2014, 136, 1815–1824

cm^{-1}, respectively. In the UVPD spectrum of the n = 2 complex (Figure 1c), no band is seen below 36 267 cm^{-1}. Thus, gain signals in the IR–UV spectrum measured at 36 226 cm^{-1} (Figure 4a) are due to IR absorption followed by UV absorption from vibrationally excited K^+•DB18C6•$(H_2O)_2$. The IR spectrum taken with the UV laser at 36 226 cm^{-1} should thus contain IR bands of all conformers present in the ion trap. The IR spectrum taken with the UV set on the sharp band at 36 326 cm^{-1} shows depletion bands at 3452, 3601, and 3721 cm^{-1} and a weak bump at ~3710 cm^{-1}. These spectral features are similar to those of the gain spectrum in Figure 4a. However, the IR–UV spectrum at 36 267 cm^{-1} (Figure 4c) provides slight different shapes from the IR spectrum at 36 326 cm^{-1} (Figure 4b); the IR spectrum in Figure 4c shows gain and depletion signals around 3720 cm^{-1}. Because the vibronic band at 36 267 cm^{-1} is quite weak, the conformer associated with this band is a minor one for the n = 2 complex. The IR spectrum measured with the UV at 36 267 cm^{-1} is likely to be affected by the gain signal due to the absorption of the main conformer. Hence, the gain signal around 3720 cm^{-1} in Figure 4c is probably due to the main conformer associated with the strong UV band at 36 326 cm^{-1}. In addition, there is a very small but noticeable difference in the position of the H-bonded OH stretch between the spectra in parts b and c of Figure 4 (3452 and 3454 cm^{-1}, respectively). We thus conclude from the IR–UV results in Figure 4 that there are at least two conformers that have very similar IR spectra. Figure 4d–j illustrates the IR spectra calculated for stable conformers of n = 2 (K2a–K2g), the structures of which are shown in Figures 3 and 4S of the Supporting Information. Among these conformers, K2d and K2f (Figure 4g, i) have a strong band around 3450 cm^{-1}, similar to the IR–UV spectra. In both of these conformers the two H_2O molecules form a chain structure, with one of them having a direct intermolecular bond with the K^+ ion. Similar to the case of the n = 1 ion, K2d, which has the H_2O molecules bound on top of DB18C6, is more stable than K2f at all the calculation levels performed in this study. Hence, we attribute the main conformer having the strong UV band at 36 326 cm^{-1} to K2d and the weak vibronic band at 36 267 cm^{-1} to K2f.

The observed and calculated IR spectra of the n = 3 complex are displayed in Figure 5. The stable conformers are shown in Figures 6 and 5S of the Supporting Information. The IR–UV spectrum measured at a nonresonant UV position (36 076 cm^{-1}, Figure 5a) shows more gain bands than the number of the OH groups of the complex, suggesting the existence of multiple conformers. These IR–UV bands are attributed to three spectra, as seen in Figure 5b–d. Figure 5b shows the IR–UV spectrum measured at the strongest UV band at 36 108 cm^{-1}. This is similar to the calculated IR spectrum of K3a (Figure 5e), which is the most stable conformer of the n = 3 ion. Therefore, the UV band at 36 108 cm^{-1} can be assigned to K3a. In K3a (Figure 6a), two H_2O molecules are directly bound to the K^+ ion and donate one OH group to the other H_2O. All the H_2O molecules are located on top of one phenyl ring of the DB18C6. The IR–UV spectra measured at 36 326 and 36 390 cm^{-1} (Figure 5c, d) have a strong IR band below 3500 cm^{-1}. In analogy with the n = 2 spectra, these IR bands can be ascribed to the H-bonded OH stretch of H_2O forming a water chain. The IR–UV spectrum at 36 326 cm^{-1} (Figure 5c) shows the H-bonded OH stretch at 3452 cm^{-1}, which is the same as that of the n = 2 conformer at 36 326 cm^{-1} (Figure 4b). This UV position in the n = 3 spectrum (36 326 cm^{-1}) coincides with that of the main conformer of n = 2 (see Figure 1c, d).

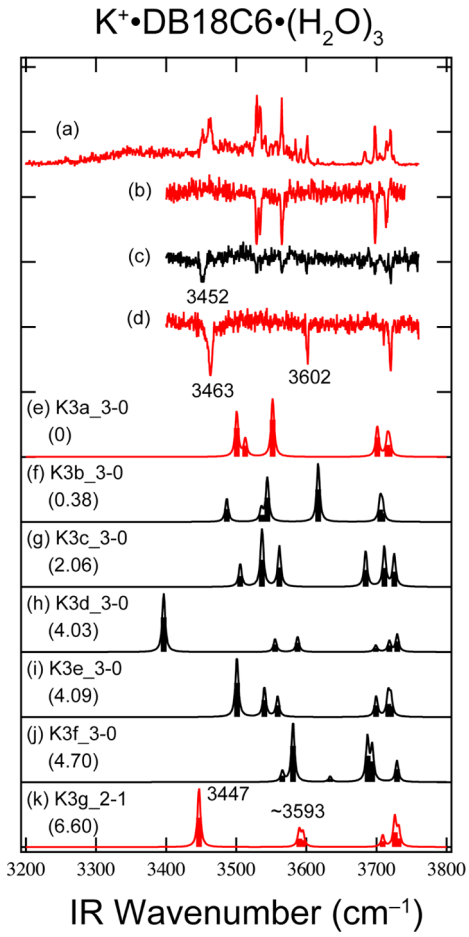

Figure 5. (a–d) IR–UV spectra of the K^+•DB18C6•$(H_2O)_3$ complex measured at the UV wavenumbers of 36 076, 36 108, 36 326, and 36 390 cm^{-1}. The UV positions at which the IR–UV spectra are measured are shown with arrows in Figure 1d. (e–k) The IR spectra calculated for stable conformers (K3a–K3g). A scaling factor of 0.9525 is employed for the vibrational frequencies calculated. The numbers in parentheses show total energies (kJ/mol) relative to that of the most stable isomer (K3a).

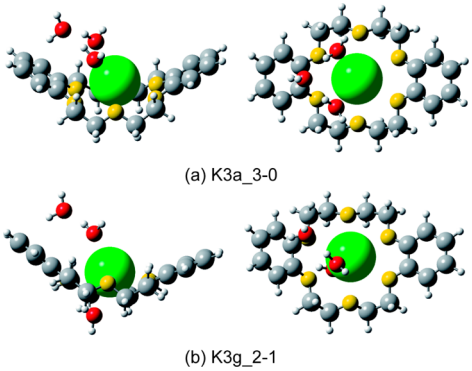

Figure 6. Side and top views of the n = 3 complex determined by the comparison of the IR spectra observed and calculated. The crown oxygen atoms are shown in yellow to distinguish them from the water ones (red).

Therefore, the 36 326 cm^{-1} band in the UV spectrum of the n = 3 ion and the IR–UV spectrum measured at this UV position (Figure 5c) can be attributed to the n = 2 complex produced by one H_2O vaporization from the mass-selected n = 3 complex

dx.doi.org/10.1021/ja4086066 | J. Am. Chem. Soc. 2014, 136, 1815–1824

between the first quadrupole and the 22-pole ion trap. Because no band is seen at 36 390 cm^{-1} in the n = 2 spectrum, the 36 390 cm^{-1} band in the UVPD spectrum of the n = 3 ion is ascribed to the intact n = 3 complex. Among the stable conformers of n = 3, K3d and K3g (Figures 6b and 5S of the Supporting Information) have H_2O chain forms. The 3602 cm^{-1} band in Figure 5d is well-reproduced by the ~3593 cm^{-1} band of K3g. Hence, the UV band of the n = 3 complex at 36 390 cm^{-1} is assigned to K3g. Conformer K3g has two H_2O molecules on the top and one at the bottom.

The IR–UV and calculated IR spectra of the n = 4 and 5 complexes are displayed in Figures 7 and 8. The stable

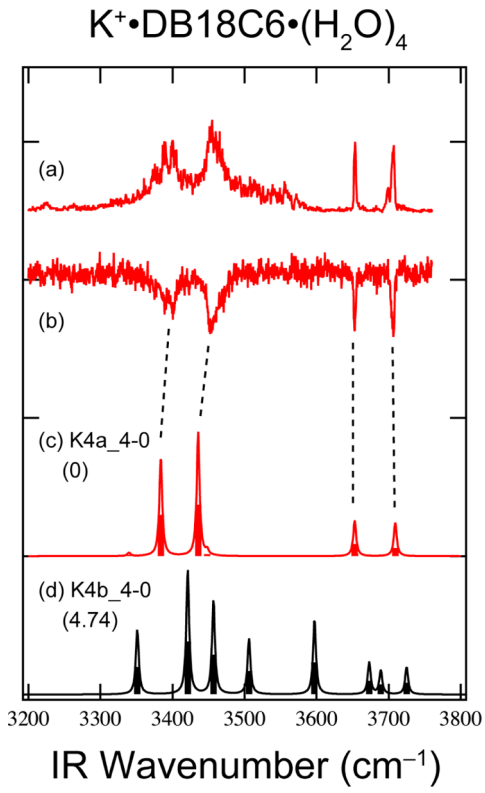

Figure 7. (a, b) IR–UV spectra of the K^+•DB18C6•$(H_2O)_4$ complex measured at the UV wavenumbers of 35 932 and 36 040 cm^{-1}. The UV positions are shown with arrows in Figure 1e. (c, d) IR spectra calculated for stable conformers (K4a and K4b). A scaling factor of 0.9525 is employed for the vibrational frequencies calculated. The numbers in parentheses show total energies (kJ/mol) relative to that of the most stable isomer (K4a).

conformers are shown in Figures 9 and 6S and 7S of the Supporting Information. There are only two and four conformers calculated below 5 kJ/mol for the n = 4 and 5 complexes, respectively. The IR gain spectra measured at nonresonant UV positions (Figures 7a and 8a) are quite similar to the depletion spectra at strong UV bands (Figures 7b and 8b), suggesting that the n = 4 and 5 complexes have only one stable conformer each. The IR–UV spectra are well-reproduced by the IR spectra calculated for the most stable conformers (K4a and K5a in Figure 9). We thus attribute the structure of the n = 4 and 5 complexes to K4a and K5a, respectively. In isomer K4a, four H_2O molecules form one ring, which is symmetrically attached on top of the K^+ ion. Also in K5a, a five-membered ring is constructed and bound to the K^+ ion and one of the oxygen atoms of DB18C6 via the H-bond.

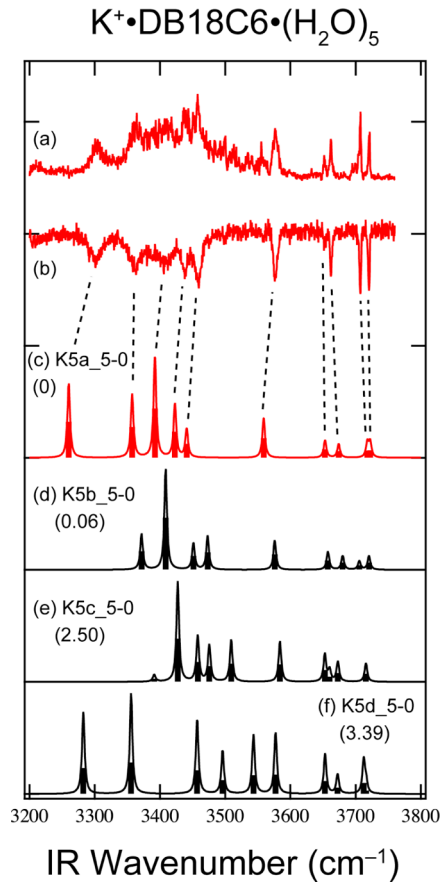

Figure 8. (a, b) IR–UV spectra of the K^+•DB18C6•$(H_2O)_5$ complex measured at the UV wavenumbers of 35 976 and 36 154 cm^{-1}. The UV positions are shown with arrows in Figure 1f. (c–f) IR spectra calculated for stable conformers (K5a–K5d). A scaling factor of 0.9525 is employed for the vibrational frequencies calculated. The numbers in parentheses show total energies (kJ/mol) relative to that of the most stable isomer (K5a).

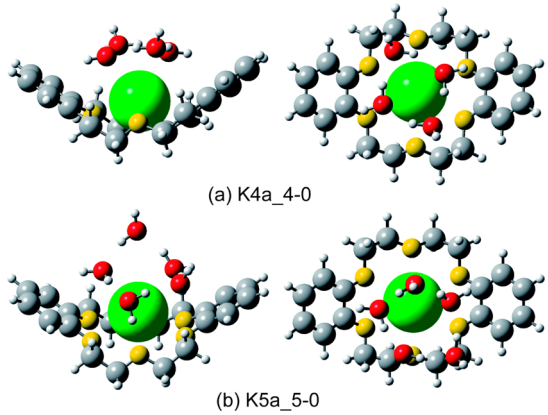

Figure 9. Side and top views of the n = 4 and 5 complexes determined by the comparison of the IR spectra observed and calculated. The crown oxygen atoms are shown in yellow to distinguish them from the water ones (red).

4. DISCUSSION

The K^+•DB18C6 complex has a boat-type C_{2v} conformer in the gas phase,[49] which is different from the symmetric D_{3d} conformation of the K^+•18C6 complex. This bent structure of K^+•DB18C6, which is due to structural constraints by the

dx.doi.org/10.1021/ja4086066 | J. Am. Chem. Soc. 2014, 136, 1815–1824

two benzene rings, affects the manner in which it is hydrated. In the case of the n = 1 complex, two types of conformers (K1a and K1b) are predicted by the calculations to be stable, with the H_2O molecule bound on top in the former and on the bottom in the latter (Figures 3 and 3S of the Supporting Information). Conformer K1a is more stable than K1b at all levels of calculation performed in this study. Figure 10a displays the

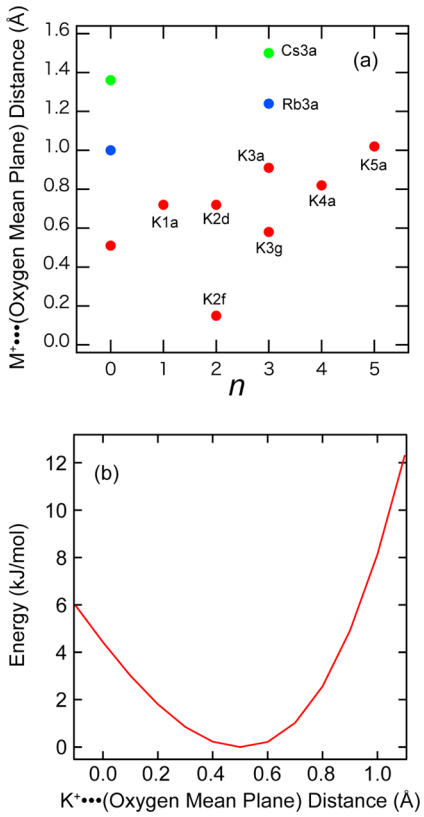

Figure 10. (a) Distance between the metal ion and the mean plane of the oxygen atoms of DB18C6 for the optimized structures of K^+•DB18C6•$(H_2O)_n$ (n = 0–5), Rb^+•DB18C6•$(H_2O)_n$ (n = 0, 3), and Cs^+•DB18C6•$(H_2O)_n$ (n = 0, 3). The values of the n = 0 complexes are taken from ref 50. (b) The potential energy curve of the K^+•DB18C6 complex as a function of the distance between the K^+ ion and the mean plane of the oxygen atoms of DB18C6 calculated at the M05-2X/6-31+G(d) level. In the calculations, the structure of the DB18C6 part is frozen.

distance between the metal ions and the oxygen mean plane of DB18C6 in the K^+•DB18C6•$(H_2O)_n$, Rb^+•DB18C6•$(H_2O)_n$, and Cs^+•DB18C6•$(H_2O)_n$ complexes. The attachment of one H_2O molecule on the top in K1a enlarges this distance from 0.51 (n = 0) to 0.72 Å. In contrast, K1b has a shorter distance (0.13 Å, not shown in Figure 10a) than that of the n = 0 complex because the H_2O molecule is bonded on the bottom side of the K^+•DB18C6 component and attracts the K^+ ion. However, the K^+•••O_{water} distance is almost the same for K1a (2.72 Å) and K1b (2.71 Å). It therefore seems that both K1a and K1b are stabilized by optimizing the distance between K^+ and H_2O at the expense of the interaction between K^+ and DB18C6. Figure 10b displays the potential energy curve of the K^+•DB18C6 complex as a function of the distance between the K^+ ion and the oxygen mean plane of DB18C6; the energy of K^+•DB18C6 is calculated at the M05-2X/6-31+G(d) level, freezing the conformation of the DB18C6 part. The potential curve has a minimum around 0.5 Å, which corresponds to the stable form of the K^+•DB18C6 complex. From this potential, the difference in the energy at 0.72 Å (K1a) and 0.13 Å (K1b) is estimated to be 1.43 kJ/mol, which indicates that the K^+•DB18C6 component in K1a is 1.43 kJ/mol more stable than that in K1b. We thus attribute the larger stability of K1a over K1b principally to the stability of the K^+•DB18C6 component in these conformers. The energy difference between K1a and K1b is calculated to be 2.60 kJ/mol (see Figure 3S of the Supporting Information), which is larger than the 1.43 kJ/mol estimated from the displacement of the metal ion relative to the crown ether. This is probably due to the interaction between H_2O and one of the benzene rings in K1a (Figure 3a). A similar argument can reasonably explain the relative stability of conformers K2d and K2f of the n = 2 complex; K2d is more stable than K2f at all levels of calculation. These conformers have a chain of H_2O molecules, and the K^+•••O_{water} distance of K2d (2.65 Å) is comparable to that of K2f (2.69 Å). Therefore, the major difference in the structure between K2d and K2f is the hydration site, similar to the difference between K1a and K1b. As shown in Figure 10a, K2d and K2f have K^+•••(oxygen mean plane of DB18C6) distances of 0.72 and 0.15 Å, respectively. According to the potential curve in Figure 10b, the difference in the energy at 0.72 and 0.15 Å is estimated to be 1.19 kJ/mol. This is almost the same as the difference in the total energy between K2d and K2f (~1.2 kJ/mol, see Figure 4S of the Supporting Information). The preference of K2d over K2f thus seems to originate from its more favorable conformation of the K^+•DB18C6 part of the complex.

As mentioned above, the spectra of the n = 3 complex indicate the presence of two stable conformers in the ion trap. This is characteristic of the K^+ complex compared to the Rb^+ and Cs^+ complexes. The measured and calculated IR spectra of the Rb^+•DB18C6•$(H_2O)_3$ and Cs^+•DB18C6•$(H_2O)_3$ complexes are shown in Figure 11. (The UVPD spectra of these complexes are displayed in the Supporting Information, Figure 1S.) The IR–UV gain spectra in Figure 11a and d, which are measured at nonresonant UV positions, are similar to the IR–UV depletion spectra monitored at strong vibronic bands (Figure 11b and e). This indicates that there is only one conformer for each of the Rb^+•DB18C6•$(H_2O)_3$ and Cs^+•DB18C6•$(H_2O)_3$ complexes. The structures of the Rb^+•DB18C6•$(H_2O)_3$ and Cs^+•DB18C6•$(H_2O)_3$ complexes are attributed to the most stable isomers, Rb3a and Cs3a, respectively, on the basis of the similarity between the IR–UV spectra and the calculated IR spectra, as shown in Figure 11. Both conformers Rb3a and Cs3a strongly resemble conformer K3a of the K^+•DB18C6•$(H_2O)_3$ complex (Figure 6a). The high stability of K3a, Rb3a, and Cs3a can be ascribed to the displaced position of the metal ions in the M^+•DB18C6 complexes. The metal ions in the nonhydrated K^+•DB18C6, Rb^+•DB18C6, and Cs^+•DB18C6 complexes deviate from the oxygen mean plane of DB18C6 by 0.51, 1.00, and 1.36 Å, respectively.[49,50] Therefore, it is quite probable that the H_2O molecules in the M^+•DB18C6•$(H_2O)_3$ complexes tend to stay above the M^+ ion to have direct intermolecular bonds with the metal ions. On the other hand, another conformer (K3g) coexists for the K^+•DB18C6•$(H_2O)_3$ complex. This is likely due to the optimum matching between the K^+ ion and the crown cavity. Compared to Rb^+ and Cs^+ ions, the K^+ ion is effectively encapsulated by DB18C6, making the interaction between K^+ and H_2O molecules weaker. As a result, structures

dx.doi.org/10.1021/ja4086066 | J. Am. Chem. Soc. 2014, 136, 1815–1824

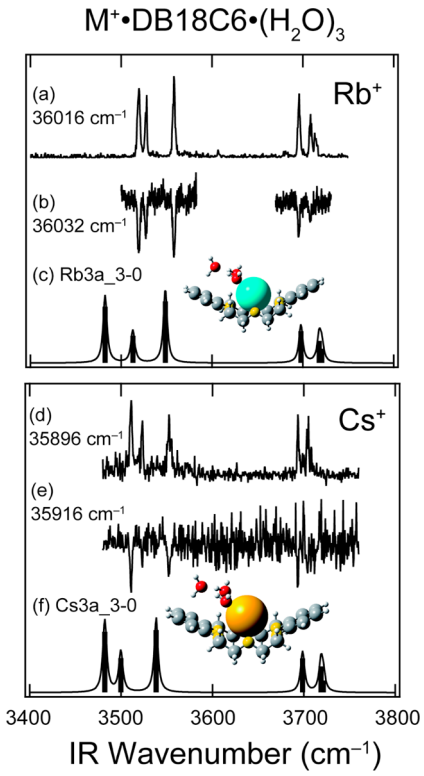

Figure 11. IR–UV spectra of the Rb^+•DB18C6•$(H_2O)_3$ (a and b) and Cs^+•DB18C6•$(H_2O)_3$ (d and e) complexes. The UV positions at which the IR–UV spectra are measured are shown with arrows in Figure 1S of the Supporting Information. (c and f) IR spectra calculated for the most stable conformers (Rb3a and Cs3a). A scaling factor of 0.9525 is employed for the vibrational frequencies calculated. The crown oxygen atoms are shown in yellow to distinguish them from the water ones (red).

with different modes of hydration, such as K3a and K3g, are less different in energy for the K^+•DB18C6 complex compared to Rb^+ and Cs^+ and can coexist. Multiple conformations for the K^+•DB18C6•$(H_2O)_3$ complex are therefore evidence of the effective capture of the K^+ ion by DB18C6 over the Rb^+ and Cs^+ ions in water. In contrast, one conformer is predominantly stable for the larger K^+•DB18C6•$(H_2O)_n$ (n = 4 and 5) complexes. In these complexes, the H_2O molecules are bound to the K^+ ion cooperatively by forming an H_2O ring, and the K^+ ion is pulled out from the DB18C6 cavity more than from the smaller complexes. In particular, the n = 4 complex has a quite symmetric structure (K4a in Figure 9a); the ring with four H_2O molecules looks the most suitable for the solvation to the K^+•DB18C6 complex. The appearance of one stable conformation for the n = 4 and 5 complexes is mainly due to the high stability of the rings formed with four or five water molecules and also due to a good matching in size between K^+ ion and these water rings.

Finally, we are left with one problem unsolved: the disagreement between the conformers found in the experiment and the order of the conformer stability obtained in the quantum chemical calculations for the n = 2 and 3 complexes. Because the IR spectra provide quite distinguishable signatures for the conformation, the determination of the complex structure based on the IR spectra should be reliable. Hence, the discrepancy originates either from the deficiency of the calculations or from the conformer formation mechanism in our experiment. To resolve this we first tried further conformational search using a different (MMFFs) force field;[59] however, we obtain only similar conformers as those in the AMBER* calculations. In addition, we calculated the total energy of the complexes at the M05-2X/6-311++G(d,p), ωB97XD/6-31+G(d), ωB97XD/6-311++G(d,p), and MP2/6-31+G(d) levels. The relative total energy is dependent on the calculation methods, but the order of the stability does not change drastically. This suggests that the disagreement originates from the formation process of the complexes in our experiment. For biomolecular ions produced in the gas phase by electrospray, the conformation is strongly dependent on the electrospray conditions.[61−63] One result characteristic of complex formation in our experiment is seen for the n = 2 complex. In the calculations of the n = 2 complexes, the conformers in which the two H_2O molecules are independently bound to K^+•DB18C6 (K2a, K2b, and K2c, Figure 4S of the Supporting Information) are predicted to be more stable than K2d, which is found in the experiment. Since K2d has an H_2O•••H_2O intermolecular bond, it is probable that conformers that have H_2O•••H_2O intermolecular bonds can be produced in the complex formation. As seen in Figure 9, the n = 4 and 5 complexes have a ring of H_2O molecules, showing a structural similarity with H_2O•••H_2O intermolecular bonds in the n = 2, 4, and 5 complexes produced in our experiment. Very recently, Russell and co-workers reported an ion mobility/mass spectrometric (IM/MS) study on the dehydration and structural evolution of hydrated Substance P (SP) ions produced by electrospray.[64] Their IM/MS results clearly reveal that the bare SP ion is produced by the charge residue model (CRM), which involves the stepwise evaporation of water from extensively hydrated clusters without major structural changes during the evaporation process. It is plausible to propose that a similar stepwise dehydration process that results in kinetic trapping of conformations that are not the lowest in energy, such as K2d, could also occur in our electrospray source. These formation processes are also similar to the ones of the K^+•18C6•$(H_2O)_n$ complexes in the gas phase via K^+ impact with 18C6–water clusters followed by water evaporation.[53] In the 22-pole ion trap, the complexes produced collide with He buffer gas many times, but these collisions do not seem to induce conformational isomerization. We observed a similar behavior in the case of small, gas-phase peptides.[65] Although the formation scheme of K2f and K3g is not clear, these conformers may be produced by the simultaneous evaporation of water clusters from relatively larger complexes. However, because the UV bands assigned to K2f (36 267 cm^{-1} in Figure 1c) and K3g (36 390 cm^{-1} in Figure 1d) are weaker than the main vibronic bands, simultaneous evaporation is thought to be a minor process.

For the K^+•DB18C6•$(H_2O)_n$ complexes, the conformers that have all the H_2O molecules on top of the K^+•DB18C6 complex appear to be more favorable. In contrast, the MD simulations of the K^+•18C6 complex in water suggested that the K^+ ion is coordinated by one H_2O molecule each from the top and bottom sides of the K^+•18C6 complex on average.[35,36] Other MD simulations of the same system show that K^+ ion in the K^+•18C6 complexes are located at the center of mass of 18C6 in water, indicating symmetric hydration.[32−36] The "asymmetric" hydration in the K^+•DB18C6•$(H_2O)_n$ complexes such as K2d, K3a, K4a, and K5a is due to intrinsic stability of the boat form for the K^+•DB18C6 component. However, this asymmetric hydration is found also for the gas-phase K^+•18C6•$(H_2O)_n$ complexes.[53,54] In addition, the existence

of conformers K2f and K3g, which have H_2O molecule(s) also at the bottom, implies that hydration on the bottom side of the K^+•DB18C6 component occurs in larger complexes, and also in solution. To shed further light on the effects of hydration on the K^+•DB18C6 encapsulation complexes, further examination of larger hydrated complexes will be indispensable.

5. SUMMARY

We have previously reported the structures of the M^+•DB18C6 and DB18C6•$(H_2O)_n$ complexes in the gas phase under cold conditions.[49−51,66,67] This spectroscopic study is a final step toward developing a more complete understanding of the ion selectivity of host species in solution, following a number of previous gas-phase studies. We have measured UV photodissociation (UVPD) and IR−UV double-resonance spectra of the K^+•DB18C6•$(H_2O)_n$ (n = 1−5) complexes produced by nanoelectrospray and cooled to ∼10 K in a 22-pole ion trap. We have determined the number and structure of the conformers of K^+•DB18C6•$(H_2O)_n$ with the aid of quantum chemical calculations. Two kinds of intermolecular interaction control the structure of the hydrated complexes: the optimum matching in size between K^+ and DB18C6 and the cooperative effect of H_2O molecules. In the n = 2 and 3 ions, there are at least two conformers each, even under the cold conditions of our ion trap. Because the crown cavity can effectively shield the K^+ ion, the hydrated complexes do not adopt one predominant hydration form, providing multiple conformations. In contrast, cooperative hydration of the K^+ ion gives only one stable conformer each for the n = 4 and 5 complexes. At present, it is difficult to predict the structure of the K^+•DB18C6 complex in water or the main factor that controls the ion selectivity in solution only from the results of this study, because two possible factors (the optimum matching in size and the cooperative effects of water molecules) seem to play a role even in the n = 2−5 complexes. However, multiple conformations observed for the K^+ complexes will have an advantage for the effective capture of the K^+ ion because of entropic effects. Previous mass spectrometric studies did not provide information on the number of conformers in the gas phase for hydrated complexes, although multiple conformation was suggested by Armentrout and co-workers for bare metal ion−ether complexes.[9,10] In this study, the cooling of the complexes provides resolved UV transitions, which enable us determine the number of conformers and measure conformer-specific IR spectra at the same time. Investigating larger gas-phase complexes with our method will provide further insight into the factor of the ion selectivity.

■ ASSOCIATED CONTENT

Supporting Information

Results of the UVPD spectra of Rb^+•DB18C6•$(H_2O)_3$ and Cs^+•DB18C6•$(H_2O)_3$, all the stable structure of the K^+•DB18C6•$(H_2O)_n$ (n = 1−5) complexes, and a full list of authors of ref 60. This material is available free of charge via the Internet at http://pubs.acs.org.

■ AUTHOR INFORMATION

Corresponding Author

y-inokuchi@hiroshima-u.ac.jp

Notes

The authors declare no competing financial interest.

■ ACKNOWLEDGMENTS

This work is partly supported by JSPS KAKENHI Grant Number 21350016 and the Swiss National Science foundation through Grant 200020_130579 and École Polytechnique Fédérale de Lausanne (EPFL). Y.I. and T.E. thank the support from JSPS through the program "Strategic Young Researcher Overseas Visits Program for Accelerating Brain Circulation".

■ REFERENCES

(1) Izatt, R. M.; Bradshaw, J. S.; Nielsen, S. A.; Lamb, J. D.; Christensen, J. J. *Chem. Rev.* **1985**, *85*, 271.
(2) Izatt, R. M.; Terry, R. E.; Haymore, B. L.; Hansen, L. D.; Dalley, N. K.; Avondet, A. G.; Christensen, J. J. *J. Am. Chem. Soc.* **1976**, *98*, 7620.
(3) Allen, F. H. *Acta Crystallogr., Sect. B: Struct. Commun.* **2002**, *58*, 380.
(4) Glendening, E. D.; Feller, D.; Thompson, M. A. *J. Am. Chem. Soc.* **1994**, *116*, 10657.
(5) Feller, D. *J. Phys. Chem. A* **1997**, *101*, 2723.
(6) Ray, D.; Feller, D.; More, M. B.; Glendening, E. D.; Armentrout, P. B. *J. Phys. Chem.* **1996**, *100*, 16116.
(7) More, M. B.; Ray, D.; Armentrout, P. B. *J. Phys. Chem. A* **1997**, *101*, 831.
(8) More, M. B.; Ray, D.; Armentrout, P. B. *J. Phys. Chem. A* **1997**, *101*, 4254.
(9) More, M. B.; Ray, D.; Armentrout, P. B. *J. Phys. Chem. A* **1997**, *101*, 7007.
(10) More, M. B.; Ray, D.; Armentrout, P. B. *J. Am. Chem. Soc.* **1999**, *121*, 417.
(11) Armentrout, P. B. *Int. J. Mass Spectrom.* **1999**, *193*, 227.
(12) Armentrout, P. B.; Austin, C. A.; Rodgers, M. T. *Int. J. Mass Spectrom.* **2012**, *330*, 16.
(13) Zhang, H.; Chu, J. H.; Leming, S.; Dearden, D. V. *J. Am. Chem. Soc.* **1991**, *113*, 7415.
(14) Zhang, H.; Dearden, D. V. *J. Am. Chem. Soc.* **1992**, *114*, 2754.
(15) Chu, I. H.; Zhang, H.; Dearden, D. V. *J. Am. Chem. Soc.* **1993**, *115*, 5736.
(16) Dearden, D. V.; Liang, Y. J.; Nicoll, J. B.; Kellersberger, K. A. *J. Mass Spectrom.* **2001**, *36*, 989.
(17) Anderson, J. D.; Paulsen, E. S.; Dearden, D. V. *Int. J. Mass Spectrom.* **2003**, *227*, 63.
(18) Maleknia, S.; Brodbelt, J. *J. Am. Chem. Soc.* **1992**, *114*, 4295.
(19) Brodbelt, J. S. *Int. J. Mass Spectrom.* **2000**, *200*, 57.
(20) Kempen, E. C.; Brodbelt, J. S. *Anal. Chem.* **2000**, *72*, 5411.
(21) Lee, S.; Wyttenbach, T.; Vonhelden, G.; Bowers, M. T. *J. Am. Chem. Soc.* **1995**, *117*, 10159.
(22) Franski, R. *Rapid Commun. Mass Spectrom.* **2009**, *23*, 3488.
(23) Franski, R. *Rapid Commun. Mass Spectrom.* **2011**, *25*, 672.
(24) Katritzky, A. R.; Malhotra, N.; Ramanathan, R.; Kemerait, R. C.; Zimmerman, J. A.; Eyler, J. R. *Rapid Commun. Mass Spectrom.* **1992**, *6*, 25.
(25) Leize, E.; Jaffrezic, A.; VanDorsselaer, A. *J. Mass Spectrom.* **1996**, *31*, 537.
(26) Malhotra, N.; Roepstorff, P.; Hansen, T. K.; Becher, J. *J. Am. Chem. Soc.* **1990**, *112*, 3709.
(27) Peiris, D. M.; Yang, Y. J.; Ramanathan, R.; Williams, K. R.; Watson, C. H.; Eyler, J. R. *Int. J. Mass Spectrom. Ion Processes* **1996**, *157*, 365.
(28) Schalley, C. A. *Int. J. Mass Spectrom.* **2000**, *194*, 11.
(29) Schalley, C. A. *Mass Spectrom. Rev.* **2001**, *20*, 253.
(30) Wipff, G.; Weiner, P.; Kollman, P. *J. Am. Chem. Soc.* **1982**, *104*, 3249.
(31) Van Eerden, J.; Harkema, S.; Feil, D. *J. Phys. Chem.* **1988**, *92*, 5076.
(32) Dang, L. X. *J. Am. Chem. Soc.* **1995**, *117*, 6954.
(33) Dang, L. X.; Kollman, P. A. *J. Am. Chem. Soc.* **1990**, *112*, 5716.
(34) Dang, L. X. *Chem. Phys. Lett.* **1994**, *227*, 211.
(35) Dang, L. X.; Kollman, P. A. *J. Phys. Chem.* **1995**, *99*, 55.

(36) Thompson, M. A.; Glendening, E. D.; Feller, D. *J. Phys. Chem.* **1994**, *98*, 10465.
(37) Zwier, M. C.; Kaus, J. W.; Chong, L. T. *J. Chem. Theory Comput.* **2011**, *7*, 1189.
(38) Hay, B. P.; Rustad, J. R.; Hostetler, C. J. *J. Am. Chem. Soc.* **1993**, *115*, 11158.
(39) Poonia, N. S. *J. Am. Chem. Soc.* **1974**, *96*, 1012.
(40) Live, D.; Chan, S. I. *J. Am. Chem. Soc.* **1976**, *98*, 3769.
(41) Bajaj, A. V.; Poonia, N. S. *Coord. Chem. Rev.* **1988**, *87*, 55.
(42) Rodriguez, J. D.; Kim, D.; Tarakeshwar, P.; Lisy, J. M. *J. Phys. Chem. A* **2010**, *114*, 1514.
(43) Martinez-Haya, B.; Hurtado, P.; Hortal, A. R.; Steill, J. D.; Oomens, J.; Merkling, P. J. *J. Phys. Chem. A* **2009**, *113*, 7748.
(44) Martinez-Haya, B.; Hurtado, P.; Hortal, A. R.; Hamad, S.; Steill, J. D.; Oomens, J. *J. Phys. Chem. A* **2010**, *114*, 7048.
(45) Hurtado, P.; Hortal, A. R.; Gámez, F.; Hamad, S.; Martínez-Haya, B. *Phys. Chem. Chem. Phys.* **2010**, *12*, 13752.
(46) Kim, H. J.; Shin, W. J.; Choi, C. M.; Lee, J. H.; Kim, N. J. *Bull. Korean Chem. Soc.* **2008**, *29*, 1973.
(47) Choi, C. M.; Kim, H. J.; Lee, J. H.; Shin, W. J.; Yoon, T. O.; Kim, N. J.; Heo, J. *J. Phys. Chem. A* **2009**, *113*, 8343.
(48) Choi, C. M.; Choi, D. H.; Heo, J.; Kim, N. J.; Kim, S. K. *Angew. Chem., Int. Ed.* **2012**, *51*, 7297.
(49) Inokuchi, Y.; Boyarkin, O. V.; Kusaka, R.; Haino, T.; Ebata, T.; Rizzo, T. R. *J. Am. Chem. Soc.* **2011**, *133*, 12256.
(50) Inokuchi, Y.; Boyarkin, O. V.; Kusaka, R.; Haino, T.; Ebata, T.; Rizzo, T. R. *J. Phys. Chem. A* **2012**, *116*, 4057.
(51) Inokuchi, Y.; Kusaka, R.; Ebata, T.; Boyarkin, O. V.; Rizzo, T. R. *ChemPhysChem* **2013**, *14*, 649.
(52) Rodriguez, J. D.; Lisy, J. M. *Int. J. Mass Spectrom.* **2009**, *283*, 135.
(53) Rodriguez, J. D.; Vaden, T. D.; Lisy, J. M. *J. Am. Chem. Soc.* **2009**, *131*, 17277.
(54) Rodriguez, J. D.; Lisy, J. M. *J. Am. Chem. Soc.* **2011**, *133*, 11136.
(55) Svendsen, A.; Lorenz, U. J.; Boyarkin, O. V.; Rizzo, T. R. *Rev. Sci. Instrum.* **2010**, *81*, 073107.
(56) Boyarkin, O. V.; Mercier, S. R.; Kamariotis, A.; Rizzo, T. R. *J. Am. Chem. Soc.* **2006**, *128*, 2816.
(57) Rizzo, T. R.; Stearns, J. A.; Boyarkin, O. V. *Int. Rev. Phys. Chem.* **2009**, *28*, 481.
(58) Nagornova, N. S.; Rizzo, T. R.; Boyarkin, O. V. *Angew. Chem., Int. Ed.* **2013**, *52*, 6002.
(59) Mohamadi, F.; Richards, N. G. J.; Guida, W. C.; Liskamp, R.; Lipton, M.; Caufield, C.; Chang, G.; Hendrickson, T.; Still, W. C. *J. Comput. Chem.* **1990**, *11*, 440.
(60) Frisch, M. J., et al. In *Gaussian 09, Revision A.1*; Gaussian, Inc.: Wallingford, CT, 2009.
(61) Nemes, P.; Goyal, S.; Vertes, A. *Anal. Chem.* **2009**, *80*, 387.
(62) Breuker, K.; McLafferty, F. W. *Proc. Natl. Acad. Sci.* **2008**, *105*, 18145.
(63) Sterling, H. J.; Cassou, C. A.; Susa, A. C.; Williams, E. R. *Anal. Chem.* **2012**, *84*, 3795.
(64) Silveira, J. A.; Fort, K. L.; Kim, D.; Servage, K. A.; Pierson, N. A.; Clemmer, D. E.; Russell, D. H. *J. Am. Chem. Soc.* **2013**, *135*, 19147.
(65) Papadopoulos, G.; Svendsen, A.; Boyarkin, O. V.; Rizzo, T. R. *J. Am. Soc. Mass Spectrom.* **2012**, *23*, 1173.
(66) Kusaka, R.; Inokuchi, Y.; Ebata, T. *Phys. Chem. Chem. Phys.* **2008**, *10*, 6238.
(67) Kusaka, R.; Inokuchi, Y.; Xantheas, S. S.; Ebata, T. *Sensors* **2010**, *10*, 3519.